Chem

CellPress

Article

Palladium-catalyzed asymmetric hydrophosphination of internal alkynes: Atroposelective access to phosphine-functionalized olefins

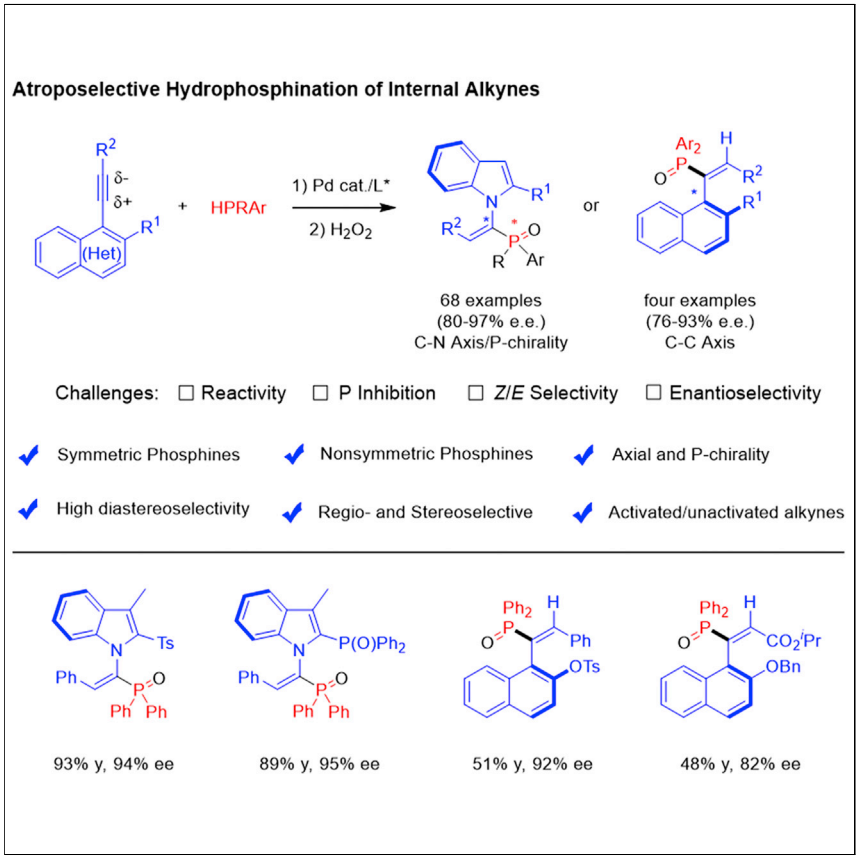

Axially chiral open-chain olefins are an underexplored class of chiral molecules, especially for trisubstituted olefins. In this work, axially chiral olefins and enantioselective hydrophosphination are integrated, and palladium-catalyzed atroposelective hydrophosphination of internal alkynes has been realized using diverse symmetrical and nonsymmetrical secondary phosphines, affording C-N axially chiral trisubstituted olefins (vinylphosphines) in excellent regioselectivity, *E*-selectivity, and enantioselectivity, as well as diastereoselectivity. The reactivity and selectivity were established via the judicious choice of a chiral bidentate ligand.

Danqing Ji, Jierui Jing, Yi Wang, ..., Xuepeng Zhang, Yong Wang, Xingwei Li

yong@nbu.edu (Y.W.)
lixw@snnu.edu.cn (X.L.)

Highlights

Atroposelective hydrophosphination of internal alkynes

Construction of axial and P-chirality

Broad reaction scope, including symmetrical and nonsymmetrical secondary phosphines

Excellent regioselectivity, *E*-selectivity, enantioselectivity, and diastereoselectivity

Ji et al., Chem *8*, 1–17
December 8, 2022
https://doi.org/10.1016/j.chempr.2022.08.019

Please cite this article in press as: Ji et al., Palladium-catalyzed asymmetric hydrophosphination of internal alkynes: Atroposelective access to phosphine-functionalized olefins, Chem (2022), https://doi.org/10.1016/j.chempr.2022.08.019

Chem

CellPress

Article

Palladium-catalyzed asymmetric hydrophosphination of internal alkynes: Atroposelective access to phosphine-functionalized olefins

Danqing Ji,[1] Jierui Jing,[1] Yi Wang,[1] Zisong Qi,[1] Fen Wang,[1] Xuepeng Zhang,[1] Yong Wang,[3,*] and Xingwei Li[1,2,4,*]

SUMMARY

Palladium-catalyzed underexplored atroposelective hydrophosphination of sterically hindered internal alkynes with secondary phosphines has been realized, affording C-N axially chiral trisubstituted olefins (vinylphosphines) in excellent regioselectivity, (*E*)-selectivity, and enantioselectivity. The axial chirality was constructed via the integration of hydrophosphination and dynamic kinetic transformation of the alkynes, with both symmetrical and nonsymmetrical secondary phosphines being applicable.

INTRODUCTION

Development of novel synthetic methods that utilize simple and abundant reagents is highly desirable toward selective construction of value-added organics. The catalytic hydrofunctionalization[1–6] of alkynes is intriguing for achieving these goals in that both substrates are widely available and readily accessible, and this transformation also features high atom and step economies. While diverse mechanistic pathways have allowed the development of numerous synthetic methods of alkyne hydrofunctionalization, the functionalized products are mostly achiral since this reaction does not directly generate a chiral carbon center. In the case of asymmetric alkyne hydrofunctionalization, enantioenriched products are often afforded via desymmetrization[7–9] of the prochiral alkyne or the coupling reagent, formation of chiral allylic compounds,[10,11] or exhaustive hydrofunctionalization to C–C single bonds.[12–14]

On the other hand, axial chirality represents a large family of chiral platforms that are widely found in numerous chiral ligands or catalysts, synthetic building blocks, and pharmaceuticals.[15–20] The majority of axially chiral molecules that have been extensively studied are biaryls.[21–23] In contrast, axially chiral olefins[24–28] have been much less explored likely due to their synthetic challenges associated with their reduced atropostability since the bonds around the open-chain C=C bond may undergo distortion to minimize the steric repulsion. The ready availability of substrates renders alkyne hyrofunctionalization an attractive strategy to address such synthetic challenges, provided that sterically internal alkynes are used and the reaction also occurs with the correct regioselectivity. However, sterically hindered alkynes generally exhibited relatively low reactivity. Consequently, atroposelective hydrofunctionalization of alkynes that affords trisubstituted chiral olefins remains a drastic challenge, especially when the products are atropomerically labile. In fact, to evade this challenge, annulative difunctionalization of alkynes has often been explored instead via well-known metal-catalyzed [2+2+2] cycloaddition,[29,30] [4+2] annulation,[31] or C–H bond activation,[32–34] but the products are typically (hetero)aromatics.

THE BIGGER PICTURE

Asymmetric hydrofunctionalization is an important chemical reaction to install functional groups at π-bonds with defined configuration and sought due to its relative atom economy. Asymmetric hydrophsophination is a specific reaction within this broader class that enables access to useful chiral phosphines. In contrast to the well-investigated asymmetric hydrophosphination reactions that deliver central chirality, access to axially chiral phosphines by this means is underexplored.

We now report Pd-catalyzed highly atroposelective hydrophosphination of internal alkynes in regio- and *E*-specificity by integration of axial chirality and hydrophosphination. Different classes of internal alkynes and symmetrical as well as nonsymmetrical secondary phosphines are applicable. In the latter case, additional P-central chirality has been constructed. This chemistry provides a new avenue to access underexplored chiral open-chain olefins and may provide new insights into underexplored atroposelective transformations of alkynes.

Please cite this article in press as: Ji et al., Palladium-catalyzed asymmetric hydrophosphination of internal alkynes: Atroposelective access to phosphine-functionalized olefins, Chem (2022), https://doi.org/10.1016/j.chempr.2022.08.019

Nevertheless, organocatalysis plays a pivotal role in atroposelective hydrofunctionalization of alkynes (Figure 1A). In 2017, Tan elegantly realized hydroalkylation of alkynals using β-diketones toward the construction of trisubstituted acroleins via the intermediacy of reactive allene species.[35] Yan[36,37] and others[38–40] developed novel organocatalyzed hydrofunctionalization of 1-alkynyl-2-naphthol analogs by taking advantage of a vinylidene *ortho*-quinone methide (VQM) intermediate. In this regime, Tan also extended the nucleophile to 2-naphthols for efficient hydroarylation.[41] Recently, Chi described N-heterocyclic carbenes (NHC)-catalyzed atroposelective synthesis of axially chiral styrenes, with selective 1,4-addition of sulfinic anion to acetylenic acylazolium intermediate as the key step.[42] In these cases, sterically hindered alkynes bearing a functional handle at the alkynyl position[35] or in the naphthol ring have been employed.[36–42] Despite the progress, the hydrofunctionalization is limited in the reaction patterns governed by the intrinsic organocatalytic modes with a handle in the sterically hindered alkyne. Thus, introduction of new heteroatoms such as phosphorus, as in hydrophosphination that deliver functional molecules, is under great demand.

The significance of chiral phosphines as ligands or catalysts has called for new asymmetric synthetic methods.[43–51] Asymmetric hydrophosphination of alkynes has been developed mostly using terminal alkynes as the substrates (Figure 1B),[52–55] and the products have been restricted to P-chirality. Besides alkynes, asymmetric hydrophosphination of activated olefins has been extensively studied since 2010 by Duan,[56,57] Leung,[58] Yin,[59,60] Zhang,[61,62] Harutyunyan and Ge,[63,64] and others using Pd, Ni, Cu, and Mn catalysts.[65–68] Chi recently also developed NHC-catalyzed hydrophsophination of α-bromoenals.[69] Moreover, enantioselective addition of P(V)-H to diverse π-bonds has been accomplished by Dong[70] and others.[71–76] In addition to unsaturated substrates, carbon and hetero electrophiles also effectively coupled with P(III)-H and P(V)-H reagents under metal catalysis.[77–87] In all these reports, the reactions are limited to the generation of C- or P-chiral centers. Of note, synthesis of the large family of axially chiral phosphines remains largely untouched via a hydrophosphination pathway. In atroposelective hydrophosphination of alkynes, the reactivity, regioselectivity, and enantioselectivity are major concerns. We reasoned that the reactivity and the regioselectivity may be partially addressed using an electronically activated and sterically hindered alkyne such as 1-alkynylindole. Nevertheless, the substrate inhibition should be fully addressed since in many cases, the PH substrate and the phosphine product may competitively bind to the catalyst.[52,53,55,59] We rationalized that the substrate inhibition and the enantioselectivity may be collectively addressed using a proper electron-rich chiral bidentate phosphine ligand that can suppress the PH binding while rendering chiral induction (Figure 1C). We now report our proof-of-concept studies on palladium-catalyzed atroposelective hydrophosphination of different classes of internal alkynes for the generation of axial and central chirality using symmetrical and nonsymmetrical secondary phosphines.

RESULTS AND DISCUSSION

We initially designed 1-alkynyl indoles bearing a proper 2-steric group as electronically activated internal alkynes for hydrphosphination studies. Thus, the 2-sulfonylindole-functionalized alkyne **1a** and Ph_2PH were selected as model substrates by palladium catalysis (Figure 2). A large set of chiral bidentate ligands were screened at 30°C. In many cases, decay of the enantioselectivity was observed as the reaction time was prolonged. Among the chiral ligands surveyed, (*S*, *S*)-BDPP, QuinoxP, and selected Josiphos ligands outperformed others and offered promising enantioselectivity in general (entries 1, 2, and 12). As expected, generally higher enantioselectivity was obtained

[1]School of Chemistry and Chemical Engineering, Shaanxi Normal University, Xi'an 710062, China

[2]Institute of Molecular Science and Engineering, Institute of Frontier and Interdisciplinary Sciences, Shandong University, Qingdao 266237, China

[3]Institute of Drug Discovery Technology, Ningbo University, Ningbo 315211, China

[4]Lead contact

*Correspondence: yong@nbu.edu (Y.W.), lixw@snnu.edu.cn (X.L.)

https://doi.org/10.1016/j.chempr.2022.08.019

Please cite this article in press as: Ji et al., Palladium-catalyzed asymmetric hydrophosphination of internal alkynes: Atroposelective access to phosphine-functionalized olefins, Chem (2022), https://doi.org/10.1016/j.chempr.2022.08.019

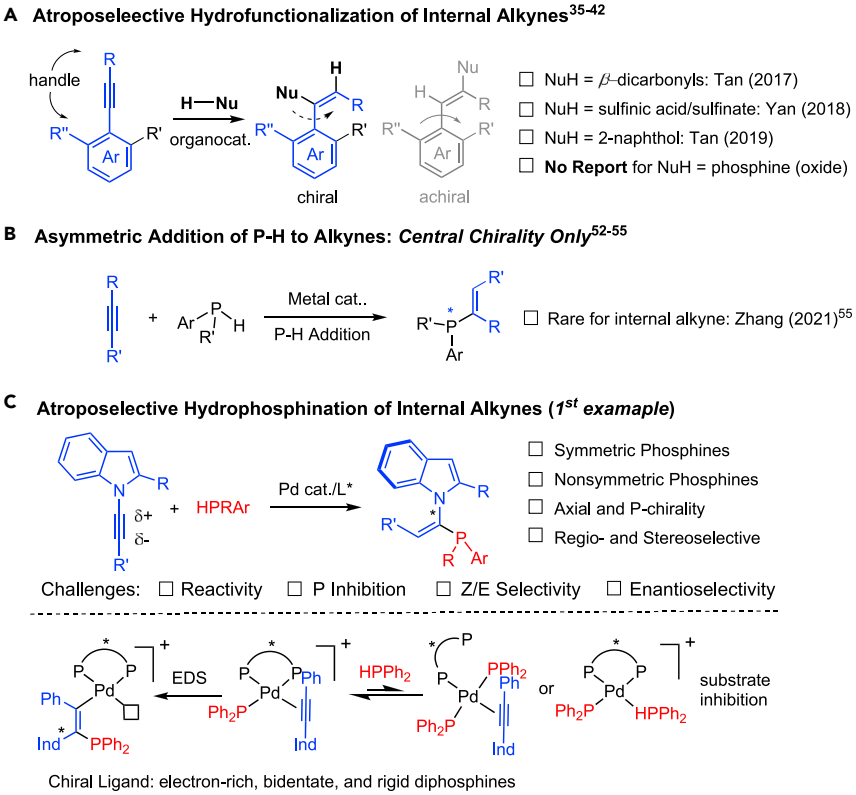

Figure 1. Asymmetric alkyne hydrofunctionalization

(A) Atroposelective hydrofunctionalization of internal alkynes.

(B) Asymmetric addition of P-H to alkynes.

(C) Atroposelective hydrophosphination of internal alkynes.

when an electron-rich (R_P, *R*)-Josiphos SL-J003-1 (**L12**) was used (entry 12). Screening of the palladium source indicated that $Pd(acac)_2$ was superior in terms of enantioselectivity (entries 15–17). Evaluation of solvents returned PhMe or PhCl as the more suitable ones (entries 18–20). Introduction of CsOAc further improved the enantioselectivity to 94%, and the product was isolated in excellent yield (entry 22). Other acid or base additives tended to give inferior results (entries 21, 23, and 24). The direct hydrophosphination product **3′** turned out to be moderately stable under air at ambient temperature, and it was converted to the oxide for convenience of characterization.

Having established of the optimal reaction conditions, we next explored the scope and generality of this coupling system (Figure 3A). Under the standard conditions, a broad scope of 1-indolylalkynes has been defined. The 3-unsubstituted indolyl substrate also reacted efficiently with slightly reduced enantioselectivity (**4**, 91% ee). Variation of the 3-substituent to benzyl or ethyl group was also successful (**5** and **6**). Various substituents such as alkyl, halogen, and methoxy at the 3-, 4-, and 5-positions of the indole ring were compatible (**7**–**13**, 88%–94% ee). The absolute configuration of the product **12** was determined to be (*S*) by X-ray crystallographic analysis (CCDC 2126532). Extension of the alkyne terminus to phenyl groups bearing various electron-donating, electron-withdrawing, and halogen substituents at the *meta* and *para* positions and to a 2-naphthyl group proved successful (**14**–**20**, 86%–93% ee). A 2-fluorophenyl group was also compatible, affording the expected product **21** in 85% ee. The presence of a 2-thienyl group gave the product **22** in high yield albeit with lower enantioselectivity (81% ee). Significantly, extension of the

Please cite this article in press as: Ji et al., Palladium-catalyzed asymmetric hydrophosphination of internal alkynes: Atroposelective access to phosphine-functionalized olefins, Chem (2022), https://doi.org/10.1016/j.chempr.2022.08.019

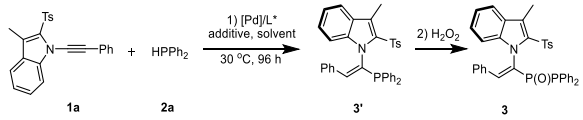

Entry	[Pd]	L*	Additive	Solvent	Yield (%)	Ee (%)
1	$Pd(acac)_2$	**L1**	-	PhMe	61	81
2	$Pd(acac)_2$	**L2**	-	PhMe	85	91
3	$Pd(acac)_2$	**L3**	-	PhMe	59	<5
4	$Pd(acac)_2$	**L4**	-	PhMe	82	79
5	$Pd(acac)_2$	**L5**	-	PhMe	58	46
6	$Pd(acac)_2$	**L6**	-	PhMe	56	33
7	$Pd(acac)_2$	**L7**	-	PhMe	63	57
8	$Pd(acac)_2$	**L8**	-	PhMe	46	38
9	$Pd(acac)_2$	**L9**	-	PhMe	46	62
10	$Pd(acac)_2$	**L10**	-	PhMe	54	18
11	$Pd(acac)_2$	**L11**	-	PhMe	61	39
12	$Pd(acac)_2$	**L12**	-	PhMe	88	92
13	$Pd(acac)_2$	**L13**	-	PhMe	89	85
14	$Pd(acac)_2$	**L14**	-	PhMe	56	20
15	$Pd(NO_3)_2{\cdot}H_2O$	**L12**	-	PhMe	80	87
16	$Pd(OH)_2$	**L12**	-	PhMe	71	88
17	$Pd(OAc)_2$	**L12**	-	PhMe	81	92
18	$Pd(acac)_2$	**L12**	-	THF	64	75
19	$Pd(acac)_2$	**L12**	-	EtOAc	75	92
20	$Pd(acac)_2$	**L12**	-	PhCl	63	92
21	$Pd(acac)_2$	**L12**	AgOAc	PhMe	89	88
22	$Pd(acac)_2$	**L12**	CsOAc	PhMe	93	94
23	$Pd(acac)_2$	**L12**	$PhCO_2H$	PhMe	59	74
24	$Pd(acac)_2$	**L12**	$Zn(OAc)_2$	PhMe	77	93

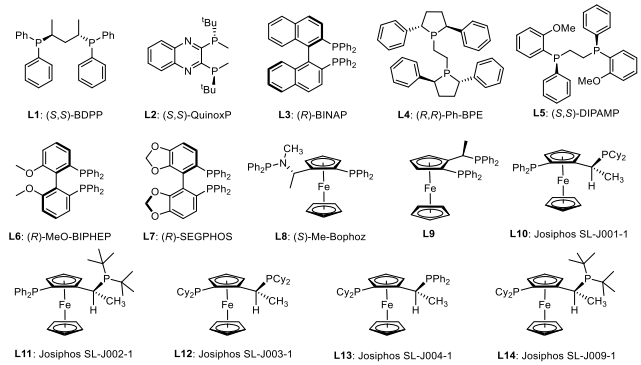

Figure 2. Optimization of reaction conditions[a]

[a]Reaction conditions: **1a** (0.1 mmol), **2a** (0.2 mmol), Pd catalyst (6 mol %), chiral ligand (9 mol %), and additive (0.3 equiv) in PhMe (2 mL), 30°C, 96 h; then H_2O_2 at 0°C for 20 min. Isolated yield. The enantiomeric excess (ee) was determined by HPLC analysis using a chiral stationary phase. See also Tables S1–S5.

substituent to alkyl (**23** and **25**) and cyclopropyl group (**24**) met with no difficulty, and the products were all isolated in excellent enantioselectivities, suggesting tolerance of the electronic effect of the alkyne. As expected, the coupling of a cyclohexenyl-substituted alkyne with $PHPh_2$-afforded product **26** in high enantioselectivity. The 2-sulfonyl group in the indole functions as an activating group as well as a bulky group to ensure axial chirality. Extension of the Ts group to other arenesulfonyls was successful (**27**–**29**, 88%–93% ee). Extension of the 2-sulfonyl group to an ester met with failure under the standard reaction conditions, under which the ee of the

Please cite this article in press as: Ji et al., Palladium-catalyzed asymmetric hydrophosphination of internal alkynes: Atroposelective access to phosphine-functionalized olefins, Chem (2022), https://doi.org/10.1016/j.chempr.2022.08.019

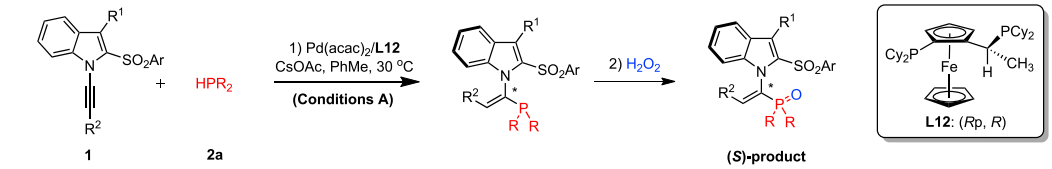

A *Scope of the Alkyne*

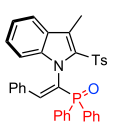

3, 93% y, 94% ee
90% y, -94% ee
(with *ent*-**L12**)

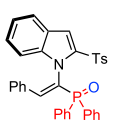

4, 73% y, 91% ee

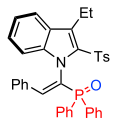

5, 91% y, 94% ee

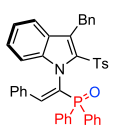

6, 92% y, 96% ee

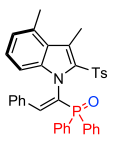

7, 64% y, 92% ee

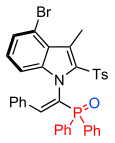

8, 59% y, 92% ee

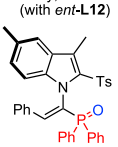

9, 95% y, 93% ee

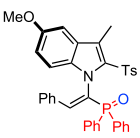

10, 86% y, 93% ee

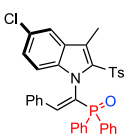

11, 89% y, 92% ee

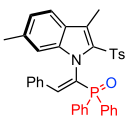

12, 83% y, 94% ee
(CCDC 2126532)

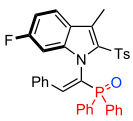

13, 83% y, 88% ee

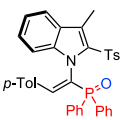

14, 93% y, 92% ee

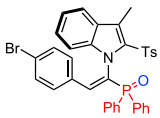

15, 76% y, 91% ee

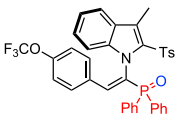

16, 75% y, 94% ee

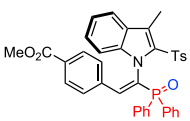

17, 85% y, 86% ee

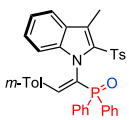

18, 93% y, 90% ee

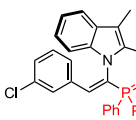

19, 89% y, 91% ee

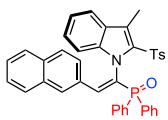

20, 89% y, 93% ee

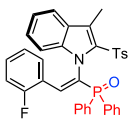

21, 72% y, 85% ee

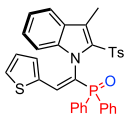

22, 87% y, 81% ee

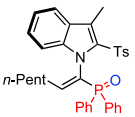

23, 90% y, 94% ee

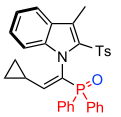

24, 92% y, 94% ee

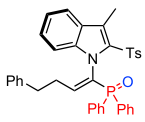

25, 81% y, 95% ee

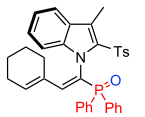

26, 64% y, 84% ee

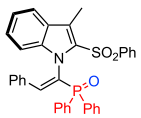

27, 82% y,93% ee

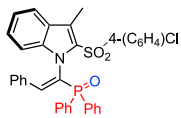

28, 90% y,88% ee

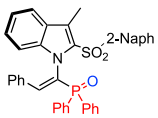

29, 83% y, 89% ee

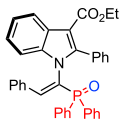

30, 68% y, 82% ee
(Conditions B)

B *Scope of Symmetric Phosphines*

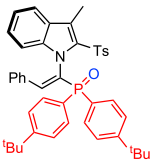

31, 91% y, 93% ee

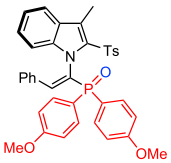

32, 82% y, 92% ee

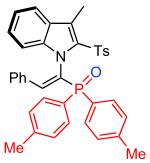

33, 90% y, 93% ee

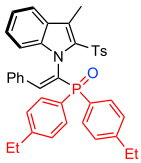

34, 81% y, 94% ee

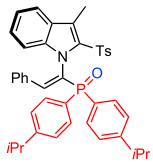

35, 78% y, 93% ee

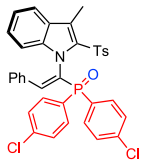

36, 61% y, 93% ee

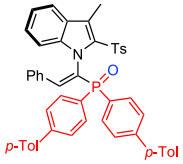

37, 84% y, 94% ee

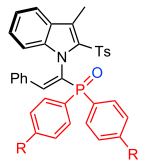

38 (R = Ph) 81% y, 96% ee
39 (R = CF_3) 81% Y, 91% ee

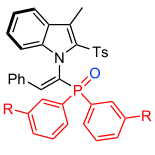

40 (R = Et) 86% y, 93% ee
41 (R = F) 84% y, 93% ee

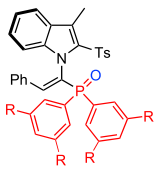

42 (R = CF_3) 68% y, 88% ee
43 (R = Me) 89% y, 93% ee

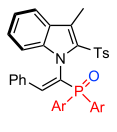

Ar = 2-MeO(C_6H_4)
44, 36% y, 89% ee

45, 82% y, 91% ee

Please cite this article in press as: Ji et al., Palladium-catalyzed asymmetric hydrophosphination of internal alkynes: Atroposelective access to phosphine-functionalized olefins, Chem (2022), https://doi.org/10.1016/j.chempr.2022.08.019

Figure 3. Scope of symmetric secondary phosphines in enantioselective hydrophosphination of alkynes

[a]Reaction conditions A: **1** (0.1 mmol), **2a** (0.2 mmol), $Pd(acac)_2$ (6 mol %), CsOAc (30 mol %), and **L12** (9 mol %) in toluene (2 mL), 30°C, 96 h. Isolated yield. The ee was determined by HPLC analysis.

[b]Conditions B: indolylphenylacetylene (0.1 mmol), **2a** (0.2 mmol), $Pd(acac)_2$ (6 mol %), and (*R*, *R*)-Ph-BPE (9 mol %) in toluene (2 mL), 0°C, 96 h.

coupled product decayed significantly versus reaction time. Moving the chiral ligand to (*R*, *R*)-Ph-BPE 0°C afforded the product **30** in good yield and in 82% ee, and the configuration of **30** has been established by electronic circular dichroism (ECD) spectroscopy (see Figure S1). The atropostability of product **3** has been examined, from which $\Delta G^{\neq}_{rac} \geq 33.4$ kcal/mol was estimated (essentially no decay of ee for 16 h at 100°C. In addition, a lower barrier of racemization ($\Delta G^{\neq}_{rac} = 30.2$) has been determined for the corresponding phosphine **3′** (80°C, PhMe) (see supplemental information [experimental section]).

The scope of the symmetric diarylphosphines was next explored in the coupling with alkyne **1a** (Figure 3B). Diarylacetylenes bearing diverse electron-donating and electron-withdrawing groups at the *para* position all reacted smoothly under the standard conditions (**31**–**39**, 91%–96% ee). Phosphines bearing different *meta*-substituted and 1,3-disubstituted phenyls also reacted in excellent enantioselectivity (**40**–**43**, 88%–93% ee). Sluggish reaction was found for *ortho*-substituted diarylphosphines due to the steric effect. Nevertheless, *ortho*-methoxy-substituted diphenylphosphine coupled in acceptable yield with high enantioselectivity (**44**, 89% ee). The secondary phosphine substrate is not limited to diarylsubstitution, and dibenzylphisphine reacted smoothly under the standard conditions A to give the product **45** in high yield and excellent enantioselectivity. Unfortunately, other dialkylphosphines such as Cy_2PH and tBu_2PH were completely inactive after extensive attempts.

Having established the scope of symmetrical phosphines, we next moved to coupling using nonsymmetrical secondary phosphines, which will generate both axial and P-chirality (Figure 4). The HPPhMes bearing two sterically biased groups was evaluated, and its coupling with alkyne **1a** was extensively screened. Our previous catalyst system turned out to be inapplicable. After various studies, a bidentate (*Sp*, *S*)-Bophoz (**L8**) was identified as a superior ligand at 0°C. Thus, the coupling with **1a** afforded the product **46** in good dr (9:1) and in excellent enantioselectivity (90% ee). The scope of the alkyne was also briefly explored. It turned out that indolylalkyne bearing different substituents at the 2- and 4-positions or bearing a different sulfonyl substituent generally underwent smooth coupling in 6.5 to 9.0:1 dr and in 82%–92% ee for the major product (**47**–**53**), and similar enantioselectivity was consistently observed for both the major and minor diastereomeric products. The major product of **48** was determined to be (*S*, *S*) configuration by X-ray crystallography (CCDC 2126528), and the rest products were assigned by analogy. A comparable diastereoselectivity was observed when the indole ring is 3-unsubstituted (**54**, 88% ee). All the above initially hydrophosphinated products are reasonably air stable, but the diastereomeric products cannot be chromatographically separated unless they were oxidized. Extension of the sterically biased phosphine to phenyl-*tert*-butylphosphine was also successful, affording the product **55** in 10:1 dr and 85% ee.

To better define the scope of the alkyne, we explored another class of *N*-alkynyl indoles (Figure 5). Thus, indoles bearing a 2-phosphonyl group coupled effectively with $HPPh_2$ in excellent enantioselectivity under the modified conditions with $Fe(OAc)_2$ being an additive and with the bidentate **L1** as the chiral ligand, yielding a relatively air-stable phosphine-phosphine oxide (**56′**, CCDC 2190722) that is potentially a diphosphine precursor. The scope of this class of alkyne also turned

Please cite this article in press as: Ji et al., Palladium-catalyzed asymmetric hydrophosphination of internal alkynes: Atroposelective access to phosphine-functionalized olefins, Chem (2022), https://doi.org/10.1016/j.chempr.2022.08.019

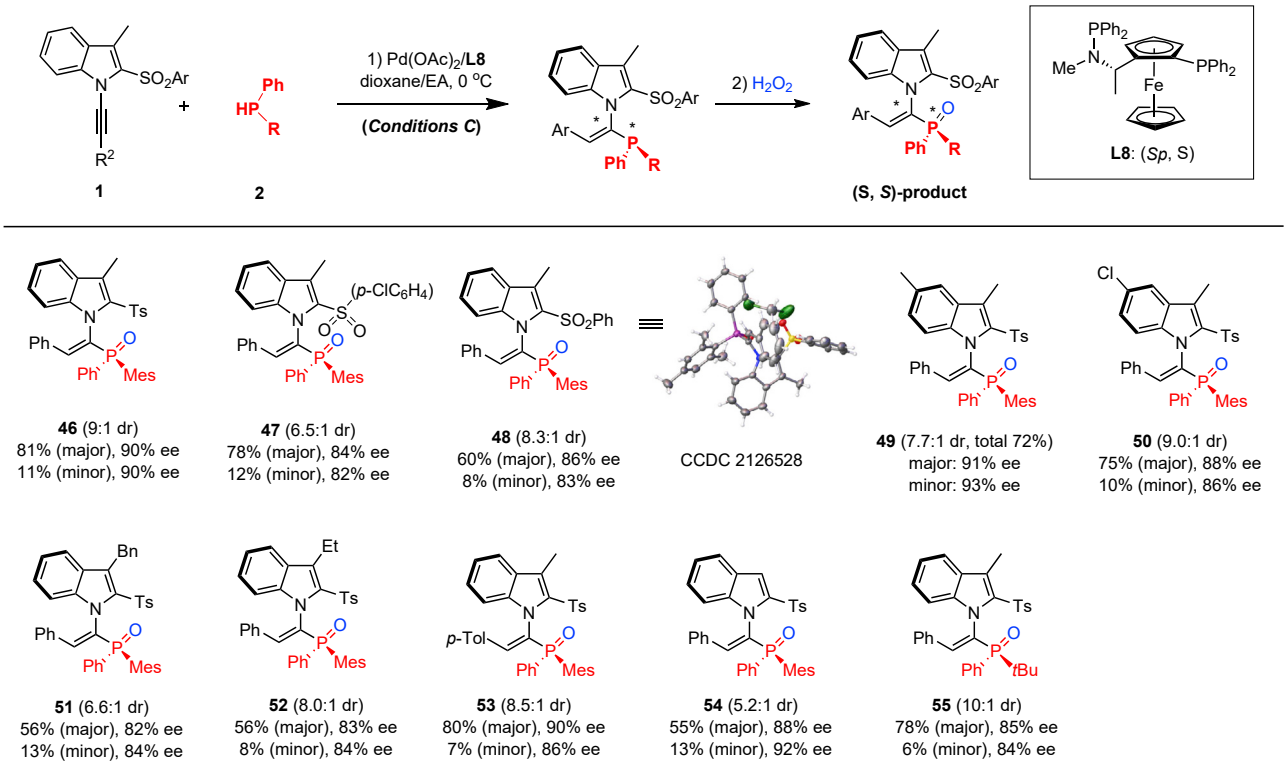

Figure 4. Scope of nonsymmetric secondary phosphines in enantioselective hydrophosphination

[a]Reactions conditions C: alkyne (0.1 mmol), nonsymmetric phosphine (0.2 mmol), $Pd(OAc)_2$ (6 mol %), and **L8** (9 mol %) in dioxane (1 mL)/EtOAc (1 mL) at 0°C, 96 h. The diastereomeric ratio (d.r.) was determined by chiral HPLC analysis.

to be broad, and both electron-donating and electron-withdrawing could be introduced to the phosphonyl group (**57**–**59**, 87%–94% ee). The alkyne terminus has also been successfully extended to several alkyl and heteroaryl groups (**61**–**63**). A decent scope of diarylphosphines has also been established with different substituents at the *meta* and *para* positions of the phenyl ring (**65**–**69**). Moreover, dibenzylphosphine also worked well under the same conditions (**70**, 80% ee). In all cases, the hydrophosphination products were isolated in 84%–97% ee. The bulky group in the alkyne has also been extended to a naphthyl ring. Thus, the coupling of a 1-alknyl-2-sulfonyloxylnaphthalene with $PHPh_2$ proceeded in high enantioselectivity although the efficiency was only low or moderate due to the lack of substrate activation (**71** and **72**, 92%–93% ee). Slightly lower enantioselectivity was also obtained for 2-OBn-sustituted substrate (**73** and **74**, 76%–82% ee). The atropostability of the phosphine-phosphine oxide **56′** has been measured. To our great surprise, a rather low activation barrier of 27.7 kcal/mol was obtained experimentally despite the larger steric effect the $P(O)Ph_2$ group compared with the Ts group. Our density functional theory (DFT) assessment of the structures of **56′** and **3′** revealed ground-state stabilization of the latter, and strong π-π stacking was detected between the T_S group and the alkenyl-phenyl ring in the product **3′**, and this tethering effect serves to increase its atropostability.[88] In addition, the C(indole)–P versus C(indole)–S bond lengths also differs (see supplemental information [experimental section and ECD spectrum of (S)-30, (R)-71, (R)-73 and DFT calculations]). This indicates that the electronic effect of the atropoisomer may contribute significantly toward the racemization barrier. In contrast, a high (>34.9 kcal/mol) racemization barrier was estimated for the diphosphine dioxide **56**. Accordingly, the high temperature required for the reduction of phosphine oxide in **56′** precluded it from being as a suitable chiral

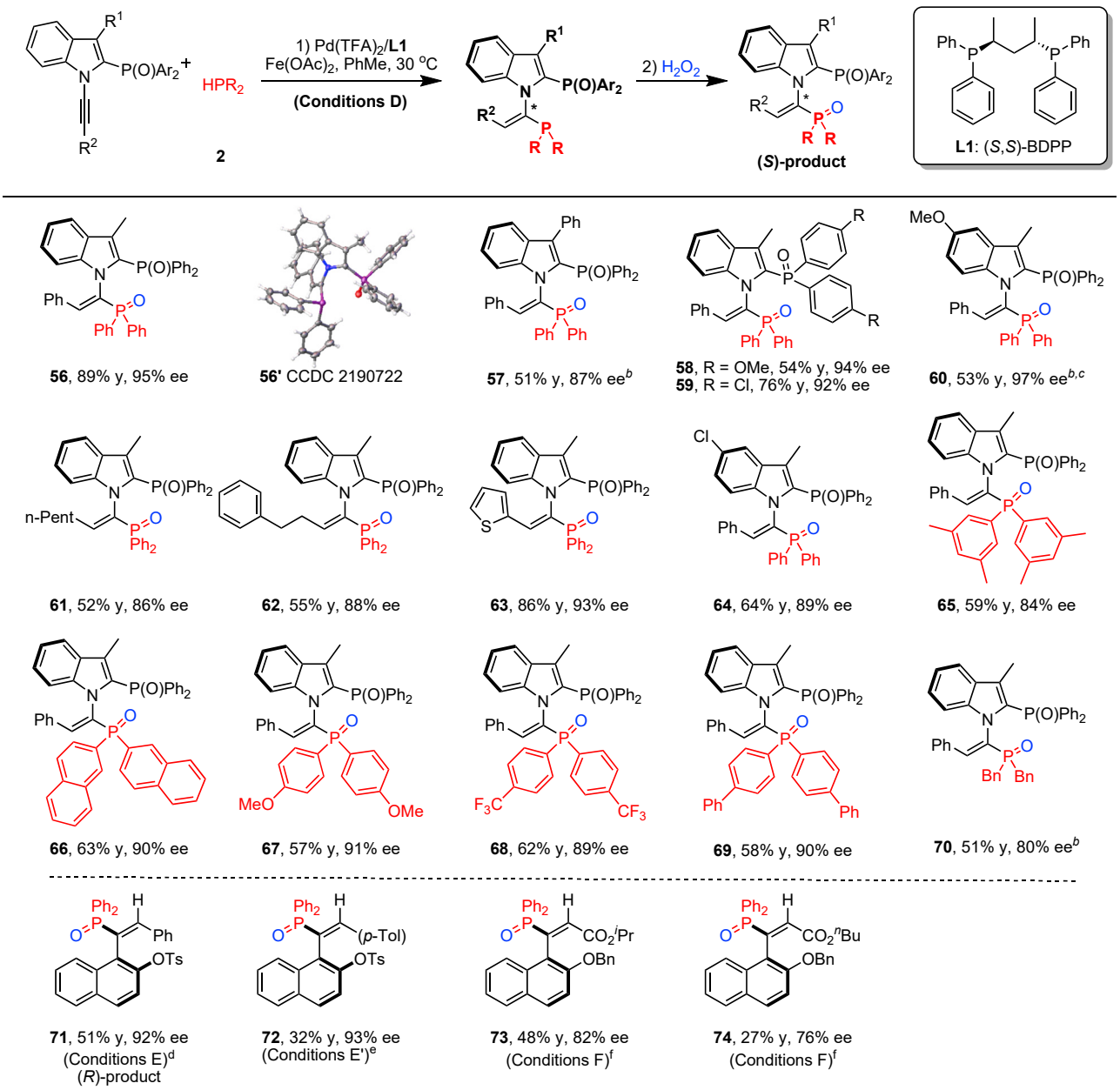

Figure 5. Scope of other classes of alkynes in hydrophosphination

(A) Reaction conditions D: **3a** (0.1 mmol), **2a** (0.2 mmol), $Pd(TFA)_2$ (6 mol %), $Fe(OAc)_2$ (30 mol %), and (*S*, *S*)-BDPP (9 mol %) in toluene (2 mL), 30°C, 96 h. Isolated yield. The ee was determined by HPLC analysis.

(B) 12 h.

(C) 20°C. See also Tables S6–S8.

(D) Reaction conditions E: 1-(2-tosyloxy)naphthyl-substituted alkyne (0.1 mmol), **2a** (0.2 mmol), $Pd(NO_3)_2 \cdot 2H_2O$ (10 mol %), $AgNO_3$ (30 mol %), and (*R*, *R*)-QuinoxP (12 mol %) in THP (2 mL), 80°C, 96 h. THP, tetrahydropyrane.

(E) Reaction conditions E′: alkyne (0.1 mmol), **2a** (0.2 mmol), $Pd(NO_3)_2 \cdot 2H_2O$ (10 mol %), Fe(OAc)2 (30 mol %), and (*R*, *R*)-QuinoxP (12 mol %) in toluene (2 mL), 80°C, 96 h. Isolated yield. The ee was determined by HPLC analysis.

(F) Conditions F: alkyne (0.1 mmol), **2a** (0.2 mmol), $Pd(acac)_2$ (10 mol %), and **L12** (12 mol %) in dichloroethane (DCE) (2 mL), 30°C, 96 h.

diphosphine ligand, and only a racemic product was obtained from the standard reduction of **56** or **56′**. In line with these observations, the hydrophosphination of a 2-phosphonylindole-functionalized alkyne devoid of the 3-methyl substituent

Please cite this article in press as: Ji et al., Palladium-catalyzed asymmetric hydrophosphination of internal alkynes: Atroposelective access to phosphine-functionalized olefins, Chem (2022), https://doi.org/10.1016/j.chempr.2022.08.019

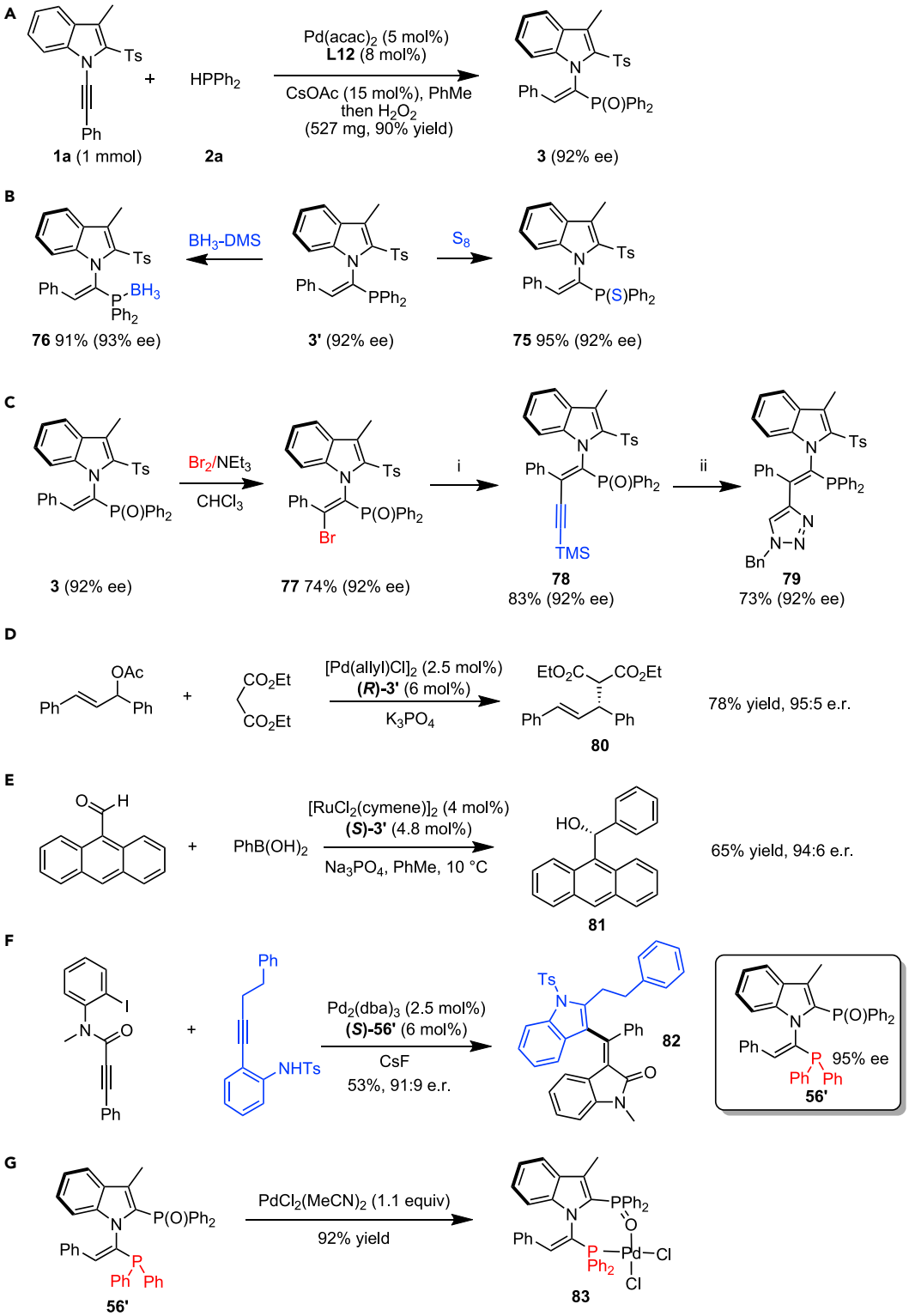

Figure 6. Synthetic applications

(A) 1 mmol scale synthesis of 3.

(B) Protect the initial hydrosphosphination product 3'.

(C) The synthesis of 79 from the product 3.

[i]TMSC≡CH, $Pd(PPh_3)_2Cl_2$ (2 mol %), CuI, PPh_3, NEt_3, 100°C.

Please cite this article in press as: Ji et al., Palladium-catalyzed asymmetric hydrophosphination of internal alkynes: Atroposelective access to phosphine-functionalized olefins, Chem (2022), https://doi.org/10.1016/j.chempr.2022.08.019

Figure 6. *Continued*
[ii](A) TBAF, (B) CuTc, BnN_3, (C) DIBAL-H.
(D) Asymmetric allylic alkylation using (R)-3′ as ligand.
(E) Asymmetric C-C coupling using (S)-3′ as ligand.
(F) Atroposelective C-C coupling using (S)-56′ as ligand.
(G) The synthesis of P-O Bidentate Pd(II) Complex 83.

only reacted with poor enantioselectivity (31% ee), possibly due to the poor stereochemical stability of the product.

Synthetic applications of representative products were next performed. The reaction of **1a** and **2a** was easily scaled up, affording product **3** in excellent yield with only slightly lower enantioselectivity (Figure 6A). In addition to the protection in the oxide form, the initial hydrosphosphination product **3′** could also be protected upon treatment with S_8 (**75**) or BH_3-DMS (**76**, Figure 6B). The olefin unit in product **3** is somewhat electronically activated. Treatment of **3** with Br_2 led to electrophilic bromination at the olefinic site, and tetrasubstituted olefin **77** was obtained in 92% ee. Alkynylation followed by dysilylation, click reaction, and standard reduction afforded a triazole-functionalized phosphine **79** that is a potential bidentate ligand (92% ee, Figure 6C). Phosphine **3′** was then designated as a chiral ligand in palladium-catalyzed asymmetric allylic alkylation of an allyl acetate, affording products **80** in high enantioselectivity (Figure 6D). In addition to palladium catalysis, ligand **3′** also worked well as a chiral ligand in Ru(II)-catalyzed asymmetric C–C coupling between a ketone and phenylboronic acid to yield the alcohol **81** in high enantioselectivity (Figure 6E). Although the enantio-enriched diphosphine failed to be obtainable from the reduction of **56**, the monophosphine **56′** may serve well as a P–O bidentate ligand. Thus, by using **56′** as a chiral bidentate ligand, an interesting Pd-catalyzed atroposelective C–C coupling has been attempted for the coupling of an alkyne-tether aryl iodide and an *o*-alkynylaniline.[89] This unprecedented double cyclization-C–C coupling reaction proceeded well in 91:9 enantiomeric ratio (e.r.) to give the desired axially chiral olefin product **82** under mild conditions (Figure 6F). In addition, treatment of $PdCl_2(MeCN)_2$ with **56′** afforded the P–O bidentate Pd(II) complex (**83**) in high yield, which could be a potentially useful chiral catalyst (Figure 6G and see supplemental information [experimental section] for the details).

Preliminary experimental studies have been conducted to explore the reaction mechanism (Figure 7). The coupling of **1a** with $DPPh_2$ afforded the product **3**-D_n with H/D exchange (~50% D) at the olefinic position (Figure 7A). This observation is consistent with a reaction pathway that involves protonolysis or sigma-bond metathesis of a palladium alkenyl intermediate. In a competitive experiment, two electronically distinguishable indolylalkynes bearing different groups at the 5-position were allowed to competitively couple with $HPPh_2$. NMR analysis indicated that the 5-methyl substrate completely overrode its 5-Cl analog, affording the product **9** in excellent yield (Figure 7B). This may suggest that a more electron-rich indole ring facilitated the coupling with more pronounced substrate activation or with stronger alkyne coordination. To explore possible phosphine inhibition, control experiments have been conducted. The employment of alkyne **1a** as a substrate toward coupling with different amounts of $HPPh_2$ afforded the product with negligible variations of the enantioselectivity with up to 10 equiv of $PHPh_2$ (48 h, Figure 7C). In contrast, appreciable decrease of the enantioselectivity was detected for the 3-unsubstituted alkyne **1a′** only in the presence of a large amount (10 equiv) of $PHPh_2$. In both cases, the reaction was significantly inhibited by 10 equiv of $PHPh_2$, suggesting substrate inhibition but probably with dechelation of

Please cite this article in press as: Ji et al., Palladium-catalyzed asymmetric hydrophosphination of internal alkynes: Atroposelective access to phosphine-functionalized olefins, Chem (2022), https://doi.org/10.1016/j.chempr.2022.08.019

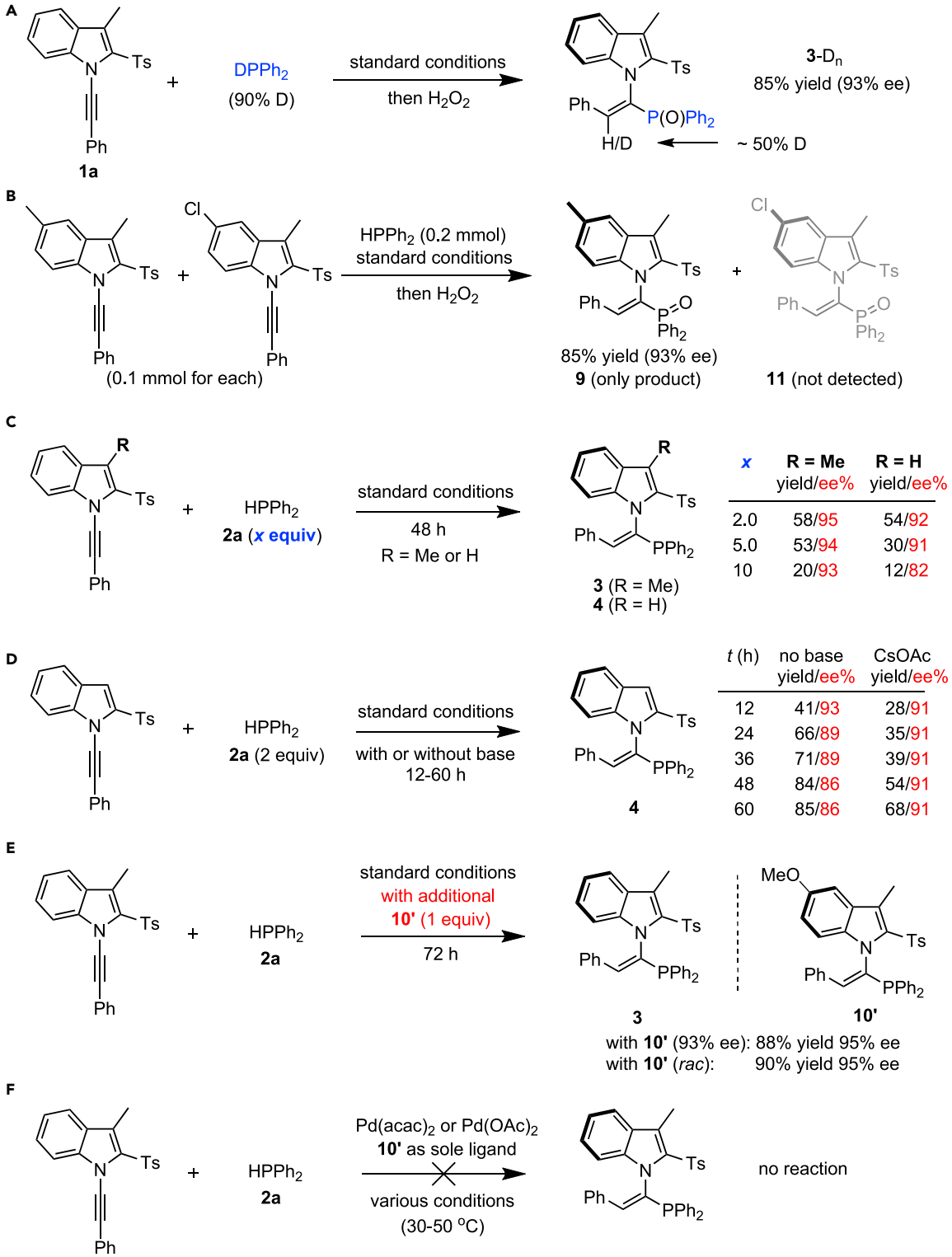

Figure 7. Mechanistic studies[a]

(A) H/D exchange experiment.

(B) Competitive reactions.

(C) Exploring possible phosphine inhibition.

(D) Control experiments to investigate the role of the base.

Please cite this article in press as: Ji et al., Palladium-catalyzed asymmetric hydrophosphination of internal alkynes: Atroposelective access to phosphine-functionalized olefins, Chem (2022), https://doi.org/10.1016/j.chempr.2022.08.019

Figure 7. *Continued*

(E) Exploring possible product inhibition.

(F) The possibility of autocatalysis of this coupling system.

[a]The ee refers to that of the trivalent phosphine product, and the yield refers to that of the phosphine oxide after H_2O_2 oxidation.

the chiral ligand only in the case of **1a′**, which is less sterically hindered and less electron rich and consequently more prone to ligand substitution-dechelation (see Figure 1C). These results highlighted the subtle steric and electronic differences of these alkynes and the importance of proper choice of a chiral bidentate ligand. The role of the base additive was then examined. It was found that the enantioselectivity of the coupling of alkyne **1a′** slightly decayed as the reaction proceeded in the absence of any base additive. Control experiments indicated that the decay was not caused by post-coupling interaction of the product with the catalyst. Introduction of CsOAc afforded a constant ee although the reaction was slightly retarded (Figure 7D). The presence of this base additive probably facilitated the formation of more coordinating PPh_2 ligand and fine-tuned the enantioselectivity. To further explore the possible product inhibition, the coupling of **1a** was conducted in the presence of an enantioenriched or a racemic phosphine product **10′** at the beginning (Figure 7E). Neither the coupling efficiency nor the enantioselectivity was essentially affected in either case, indicative of negligible phosphine product inhibition. We also attempted to apply **10′** as the sole chiral ligand for the coupling of **1a** and $PHPh_2$, but only starting materials were recovered under various conditions (Figure 7F). These observations verified the irrelevance of autocatalysis in this coupling system, and the chiral phosphine product cannot outcompete the $PHPh_2$ substrate (see supplemental information [experimental section]).

The pathway of this coupling reaction likely involves the initial deprotonation-ligand substitution between $HPPh_2$ and L*PdX_2 to give a Pd(II)PPh_2 species (Figure 8). The alkyne coordination is then followed by an enantio-determining migratory insertion of the PPh_2 group into the alkyne. This insertion is also regioselective as dictated by both the electronic and steric effects of the 1-indolyl group, which functioned in the same direction. Indeed, the metal tends to end up at the vinyl site that is distal to the bulky aryl group on the basis of our previous studies.[32–34] Protonolysis of the C–Pd bond eventually furnishes the coupled product. In the enantio-determining migratory insertion, the more hindered indole moiety of the alkyne tends to be placed downward, and two orientations (**E** and **E′** shown in Figure 8) of the alkyne versus the PPh_2 group can be visioned. In the intermediate **E**, minimal repulsion between the alkyne-attached phenyl group and the alkylphosphino group is experienced. In addition, the π-acidic alkyne is favorably *trans* to the more donating alkylphosphino group, which eventually affords the observed (*S*) selectivity.

Our DFT calculations supported this proposal (Figure 8, middle). The intermediate **E** lies 6.5 kcal/mol lower than the **E′** in free energy. Accordingly, the transition state of the major route (TS_E) was also found to be lower in free energy than the TS_E' by 7.5 kcal/mol. By investigation of the geometries (see Table S12), it was found that the interaction between the biased chelating ligand and the alkyne plays an important role. In **E′**, strong π-π interaction was observed between the PPh_2 and the alkyne-attached phenyl group. Meanwhile, the Ts side-chain of the alkyne was oriented on top of the bulky alkylphosphino group, which exerts steric effect toward ligation of the alkyne unit. While in intermediate **E**, one of the phenyl rings of the PPh_2 group formed a T-shape orientation with the phenyl of the alkyne, and this

Please cite this article in press as: Ji et al., Palladium-catalyzed asymmetric hydrophosphination of internal alkynes: Atroposelective access to phosphine-functionalized olefins, Chem (2022), https://doi.org/10.1016/j.chempr.2022.08.019

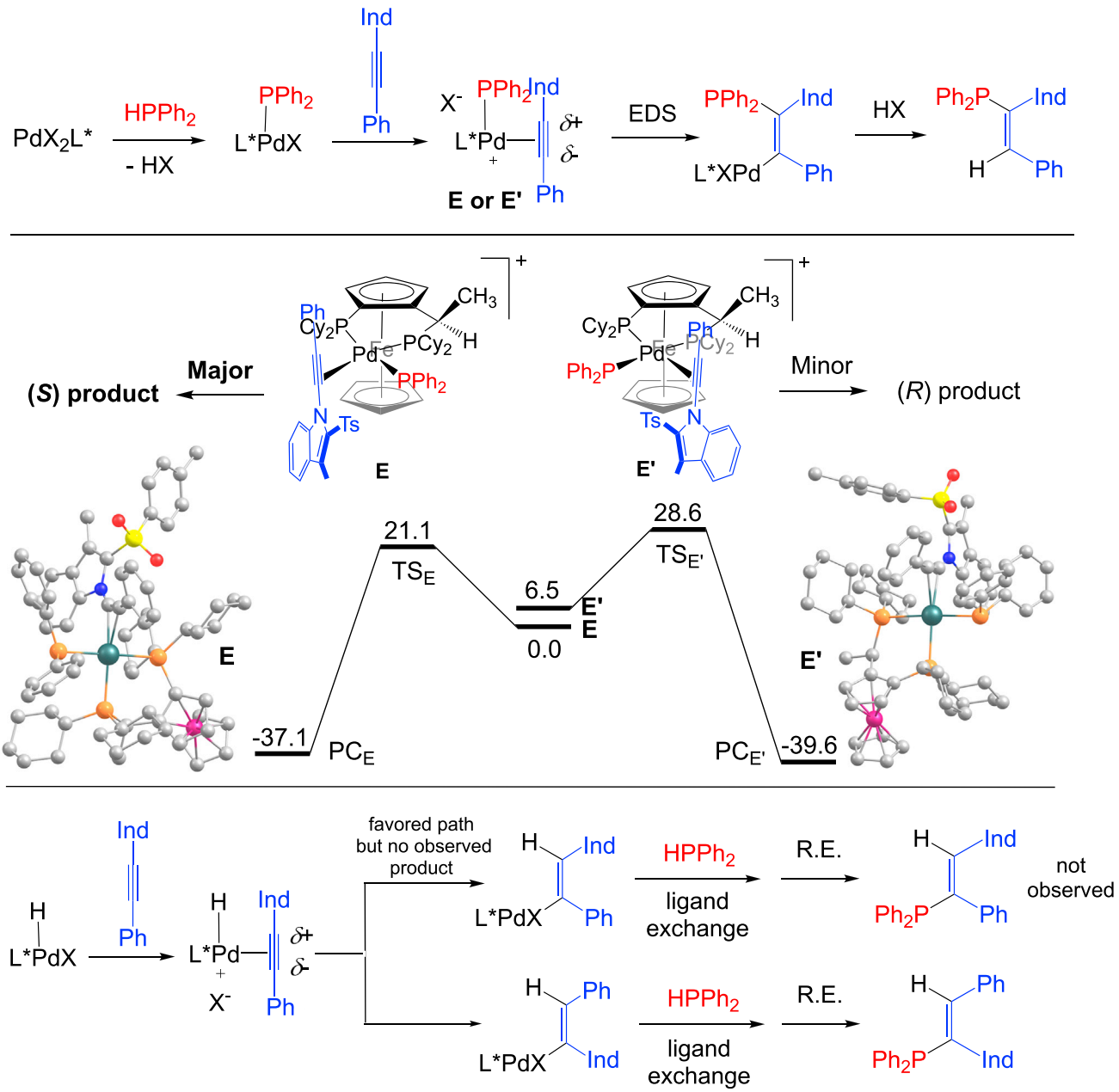

Figure 8. Proposed reaction mechanism and DFT rationalization of the enantioselectivity[a]

[a]The energy profiles (in kcal/mol) for the C–P bond formation at the UB3LYP/Lanl2tz (Pd,Fe)-6-31+G**(the rest)//Lanl2dz (Pd,Fe)-6-31G*(the rest) computational level are presented. Hydrogen atoms of the calculated geometries of **E** and **E′** were omitted for clarity. Ind, 2-substitited 1-indolyl. The anion was omitted. EDS, enantio-determining step.

caused the other phenyl group in the PPh_2 to lie between the phenyl and indole rings to avoid steric interactions, which kept the Ts side-chain away from the bulky alkylphosphino group. These different phenyl-phenyl orientations (the π-π stacking versus the T-shape) along with the different orientation of the Ts side-chain affected the coordination of the alkyne carbons (in **E**, Pd–C1: 2.243 Å, Pd–C2: 2.333 Å; in **E′**, Pd–C1: 2.331 Å, Pd–C2: 2.369 Å). Of note, the hydropalladation pathway[70,90,91] that has been suggested in alkyne hydrophosphorylation using $P(O)H(OMe)_2$ or $HP(O)Ph_2$ is unlikely because the opposite regioselectivity is

Please cite this article in press as: Ji et al., Palladium-catalyzed asymmetric hydrophosphination of internal alkynes: Atroposelective access to phosphine-functionalized olefins, Chem (2022), https://doi.org/10.1016/j.chempr.2022.08.019

expected (Figure 8, bottom). Indeed, our DFT studies verified that the opposite (unobserved) regioselectivity of insertion is more kinetically favorable by at least 13 kcal/mol (see Tables S13 and S14). This is caused by the weaker interaction between the Pd and the C(Indolyl) akynyl carbon (Pd–C(ind): ~ 2.8 angstrom) than that between the Pd–C(Ph) (Pd–C: ~2.3 angstrom) in the staring palladium hydride intermediate, which is consistent with the higher nucleophilicity/coordinating ability of the C(Ph) alkynyl site. This different binding preference causes drastically different shapes of the corresponding transition states during hydride insertion. For hydride insertion into the C(Ph) site, a triangle shape of the H-C-C-Pd moiety with large tension is observed in the transition state, while for hydride addition to the C(Indolyl), a favorable, regular quadrangle-like Pd-C-C-H transition state was identified (see supplemental information [ECD spectrum of (S)-30, (R)-71, (R)-73 and DFT calculations]).

Conclusion

In summary, we have realized palladium-catalyzed atroposelective hydrophosphination of different classes of sterically hindered internal alkynes using diverse secondary phosphines. The coupling system overcomes the low reactivity of internal alkynes via substrate activation using a sterically bulky but electron-rich 1-indolyl group with different substituents at the 2-position, affording C-N axially chiral trisubstituted olefins (vinylphosphines) in excellent regioselectivity, *E*-selectivity, and enantioselectivity under mild reaction conditions. The axial chirality was established via the integration of hydrophosphination and dynamic kinetic transformation of the alkynes, with both symmetrical and nonsymmetrical secondary phosphines, including a dibenzylphophine, being applicable. In the case of nonsymmetrical secondary phosphines, additional P-central chirality has been constructed in good diastereoselectivity as well as high enantioselectivity. The observed enantioselectivity has been rationalized by DFT studies. The hydrophosphinated products showed promising potential as chiral ligands in asymmetric catalysis. This hydrophosphination reaction offers a new approach to access underexplored chiral open-chain olefins and may provide new insight into direct atroposelective functionalization of alkynes.

EXPERIMENTAL PROCEDURES

Resource availability

Lead contact

Further information and requests for resources should be directed to and will be fulfilled by the lead contact Xingwei Li (lixw@snnu.edu.cn).

Materials availability

All materials generated in this study are available from the lead contact without restriction.

Data and code availability

The date of the X-ray crystallographic structures of **12**, **48**, and **56′** have been deposited in the Cambridge Crystallographic Data Center under accession numbers CCDC: 2126532, 2126528, and 2190722, respectively.

Methods

Full experimental procedures are provided in the supplemental information.

SUPPLEMENTAL INFORMATION

Supplemental information can be found online at https://doi.org/10.1016/j.chempr.2022.08.019.

ACKNOWLEDGMENTS

Financial supports from NSFC (22101167 and 21873052) and the SNNU are gratefully acknowledged.

AUTHOR CONTRIBUTIONS

X.L. conceived the concept and directed the project. D.J., J.J., Y.W., Z.Q., and F.W. conducted the experiments and data analysis. X.Z. and Y.W. conducted the DFT studies. X.L. and Z.Q. wrote the paper with feedback from all other authors.

DECLARATION OF INTERESTS

The authors declare no competing interests.

Received: December 14, 2021
Revised: July 21, 2022
Accepted: August 26, 2022
Published: September 23, 2022

REFERENCES

1. Alonso, F., Beletskaya, I.P., and Yus, M. (2004). Transition-metal-catalyzed addition of heteroatom-hydrogen bonds to alkynes. Chem. Rev. *104*, 3079–3159.
2. Beller, M., Seayad, J., Tillack, A., and Jiao, H. (2004). Catalytic Markovnikov and anti-Markovnikov functionalization of alkenes and alkynes: recent developments and trends. Angew. Chem. Int. Ed. Engl. *43*, 3368–3398.
3. Severin, R., and Doye, S. (2007). The catalytic hydroamination of alkynes. Chem. Soc. Rev. *36*, 1407–1420.
4. Müller, T.E., Hultzsch, K.C., Yus, M., Foubelo, F., and Tada, M. (2008). Hydroamination: direct addition of amines to alkenes and alkynes. Chem. Rev. *108*, 3795–3892.
5. Zeng, X. (2013). Recent advances in catalytic sequential reactions involving hydroelement addition to carbon-carbon multiple bonds. Chem. Rev. *113*, 6864–6900.
6. Cadierno, V. (2021). Recent advances in the transition metal-catalyzed addition of carboxylic acids to alkynes. Curr. Org. Chem. *25*, 2260–2303.
7. Mourad, A.K., Leutzow, J., and Czekelius, C. (2012). Anion-induced enantioselective cyclization of diynamides to pyrrolidines catalyzed by cationic gold complexes. Angew. Chem. Int. Ed. Engl. *51*, 11149–11152.
8. Huang, L., Yang, H.-B., Zhang, D.-H., Zhang, Z., Tang, X.-Y., Xu, Q., and Shi, M. (2013). Gold-catalyzed intramolecular regio- and enantioselective cycloisomerization of 1,1-bis(indolyl)-5-alkynes. Angew. Chem. Int. Ed. Engl. *52*, 6767–6771.
9. Zhang, Y., Zhang, F., Chen, L., Xu, J., Liu, X., and Feng, X. (2019). Asymmetric synthesis of P-stereogenic compounds via thulium(III)-catalyzed desymmetrization of dialkynylphosphine oxides. ACS Catal. *9*, 4834–4840.
10. Li, G., Huo, X., Jiang, X., and Zhang, W. (2020). Asymmetric synthesis of allylic compounds via hydrofunctionalisation and difunctionalisation of dienes, allenes, and alkynes. Chem. Soc. Rev. *49*, 2060–2118.
11. Kennemur, J.L., Maji, R., Scharf, M.J., and List, B. (2021). Catalytic asymmetric hydroalkoxylation of C-C multiple bonds. Chem. Rev. *121*, 14649–14681.
12. Cheng, Z., Guo, J., and Lu, Z. (2020). Recent advances in metal-catalysed asymmetric sequential double hydrofunctionalization of alkynes. Chem. Commun. (Camb) *56*, 2229–2239.
13. Guo, J., Cheng, Z., Chen, J., Chen, X., and Lu, Z. (2021). Iron- and cobalt-catalyzed asymmetric hydrofunctionalization of alkenes and alkynes. Acc. Chem. Res. *54*, 2701–2716.
14. Shi, S.-L., and Buchwald, S.L. (2015). Copper-catalysed selective hydroamination reactions of alkynes. Nat. Chem. *7*, 38–44.
15. Brunel, J.M. (2007). Update 1 of: BINOL: a versatile chiral reagent. Chem. Rev. *107*, PR1–PR45.
16. Parmar, D., Sugiono, E., Raja, S., and Rueping, M. (2014). Complete field guide to asymmetric BINOL-phosphate derived Brønsted acid and metal catalysis: history and classi fi cation by mode of activation; Brønsted acidity, hydrogen bonding, ion pairing, and metal phosphates. Chem. Rev. *114*, 9047–9153.
17. Akiyama, T., and Mori, K. (2015). Stronger Brønsted acids: recent progress. Chem. Rev. *115*, 9277–9306.
18. Smyth, J.E., Butler, N.M., and Keller, P.A. (2015). A twist of nature—the significance of atropisomers in biological systems. Nat. Prod. Rep. *32*, 1562–1583.
19. Wang, J., Zeng, W., Li, S., Shen, L., Gu, Z., Zhang, Y., Li, J., Chen, S., and Jia, X. (2017). Discovery and assessment of atropisomers of (±)-lesinurad. ACS Med. Chem. Lett. *8*, 299–303.
20. Toenjes, S.T., and Gustafson, J.L. (2018). Atropisomerism in medicinal chemistry: challenges and opportunities. Future Med. Chem. *10*, 409–422.
21. Liao, G., Zhou, T., Yao, Q.-J., and Shi, B.-F. (2019). Recent advances in the synthesis of axially chiral biaryls via transition metal-catalysed asymmetric C–H functionalization. Chem. Commun. (Camb) *55*, 8514–8523.
22. Carmona, J.A., Rodríguez-Franco, C., Fernández, R., Hornillos, V., and Lassaletta, J.M. (2021). Atroposelective transformation of axially chiral (hetero)biaryls. From desymmetrization to modern resolution strategies. Chem. Soc. Rev. *50*, 2968–2983.
23. Cheng, J.K., Xiang, S.-H., Li, S., Ye, L., and Tan, B. (2021). Recent advances in catalytic asymmetric construction of atropisomers. Chem. Rev. *121*, 4805–4902.
24. Zhang, Z.-X., Zhai, T.-Y., and Ye, L.-W. (2021). Synthesis of axially chiral compounds through catalytic asymmetric reactions of alkynes. Chem. Catal. *1*, 1378–1412.
25. Feng, J., and Gu, Z. (2021). Atropisomerism in styrene: synthesis, stability, and applications. SynOpen *05*, 68–85.
26. Jin, L., Yao, Q.-J., Xie, P.-P., Li, Y., Zhan, B.-B., Han, Y.-Q., Hong, X., and Shi, B.-F. (2020). Atroposelective synthesis of axially chiral styrenes via an asymmetric C-H functionalization strategy. Chem *6*, 497–511.
27. Song, H., Li, Y., Yao, Q.-J., Jin, L., Liu, L., Liu, Y.-H., and Shi, B.-F. (2020). Synthesis of axially chiral styrenes through Pd-catalyzed asymmetric C−H olefination enabled by an amino amide transient directing group. Angew. Chem. Int. Ed. *59*, 6576–6580.
28. Jin, L., Zhang, P., Li, Y., Yu, X., and Shi, B.-F. (2021). Atroposelective synthesis of conjugated

diene-based axially chiral styrenes via Pd(II)-catalyzed thioether-directed alkenyl C-H olefination. J. Am. Chem. Soc. *143*, 12335–12344.

29. Tanaka, K., Nishima, G., Wada, Z., and Noguchi, K. (2004). Enantioselective synthesis of axially chiral phthalides through cationic [$Rh^{I}(H_8$-binap)]-catalyzed cross alkyne cyclotrimerization. Angew. Chem. Int. Ed. *43*, 6510–6512.

30. Tanaka, K. (2009). Transition-metal-catalyzed enantioselective [2+2+2] cycloadditions for the synthesis of axially chiral biaryls. Chem. Asian J. *4*, 508–518.

31. Fang, Z.-J., Zheng, S.-C., Guo, Z., Guo, J.-Y., Tan, B., and Liu, X.-Y. (2015). Asymmetric synthesis of axially chiral isoquinolones: nickel-catalyzed denitrogenative transannulation. Angew. Chem. Int. Ed. Engl. *54*, 9528–9532.

32. Wang, F., Qi, Z., Zhao, Y., Zhai, S., Zheng, G., Mi, R., Huang, Z., Zhu, X., He, X., and Li, X. (2020). Rhodium(III)-catalyzed atroposelective synthesis of biaryls by C−H activation and intermolecular coupling with sterically hindered alkynes. Angew. Chem. Int. Ed. Engl. *59*, 13288–13294.

33. Wang, F., Jing, J., Zhao, Y., Zhu, X., Zhang, X.-P., Zhao, L., Hu, P., Deng, W.-Q., and Li, X. (2021). Rhodium-catalyzed C−H activation-based construction of axially and centrally chiral indenes through two discrete insertions. Angew. Chem. Int. Ed. Engl. *60*, 16628–16633.

34. Mi, R., Chen, H., Zhou, X., Li, N., Ji, D., Wang, F., Lan, Y., and Li, X. (2022). Rhodium-catalyzed atroposelective access to axially chiral olefins via C−H Bond activation and directing group migration. Angew. Chem. Int. Ed. Engl. *61*, e202111860.

35. Zheng, S.C., Wu, S., Zhou, Q., Chung, L.W., Ye, L., and Tan, B. (2017). Organocatalytic atroposelective synthesis of axially chiral styrenes. Nat. Commun. *8*, 15238.

36. Jia, S., Chen, Z., Zhang, N., Tan, Y., Liu, Y., Deng, J., and Yan, H. (2018). Organocatalytic enantioselective construction of axially chiral sulfone-containing styrenes. J. Am. Chem. Soc. *140*, 7056–7060.

37. Tan, Y., Jia, S., Hu, F., Liu, Y., Peng, L., Li, D., and Yan, H. (2018). Enantioselective construction of vicinal diaxial styrenes and multiaxis system via organocatalysis. J. Am. Chem. Soc. *140*, 16893–16898.

38. Huang, A., Zhang, L., Li, D., Liu, Y., Yan, H., and Li, W. (2019). Asymmetric one-pot construction of three stereogenic elements: chiral carbon center, stereoisomeric alkenes, and chirality of axial styrenes. Org. Lett. *21*, 95–99.

39. Li, Q.-Z., Lian, P.F., Tan, F.-X., Zhu, G.-D., Chen, C., Hao, Y., Jiang, W., Wang, X.-H., Zhou, J., and Zhang, S.-Y. (2020). Organocatalytic enantioselective construction of heterocycle-substituted styrenes with chiral atropisomerism. Org. Lett. *22*, 2448–2453.

40. Wang, C.-S., Li, T.-Z., Liu, S.-J., Zhang, Y.-C., Deng, S., Jiao, Y., and Shi, F. (2020). Axially chiral aryl-alkene-indole framework: a nascent member of the atropisomeric family and its catalytic asymmetric construction. Chin. J. Chem. *38*, 543–552.

41. Wang, Y.-B., Yu, P., Zhou, Z.-P., Zhang, J., Wang, J., Luo, S.-H., Gu, Q.-S., Houk, K.N., and Tan, B. (2019). Rational design, enantioselective synthesis and catalytic applications of axially chiral EBINOLs. Nat. Catal. *2*, 504–513.

42. Yan, J.-L., Maiti, R., Ren, S.-C., Tian, W., Li, T., Xu, J., Mondal, B., Jin, Z., and Chi, Y.R. (2022). Carbene-catalyzed atroposelective synthesis of axially chiral styrenes. Nat. Commun. *13*, 84.

43. Tang, W., and Zhang, X. (2003). New chiral phosphorus ligands for enantioselective hydrogenation. Chem. Rev. *103*, 3029–3070.

44. Xie, J.-H., and Zhou, Q.-L. (2008). Chiral diphosphine and monodentate phosphorus ligands on a spiro scaffold for transition-metal-catalyzed asymmetric reactions. Acc. Chem. Res. *41*, 581–593.

45. Ye, L.-W., Zhou, J., and Tang, Y. (2008). Phosphine-triggered synthesis of functionalized cyclic compounds. Chem. Soc. Rev. *37*, 1140–1152.

46. Fernández-Pérez, H., Etayo, P., Panossian, A., and Vidal-Ferran, A. (2011). Phosphine-phosphinite and phosphine-phosphite ligands: preparation and applications in asymmetric catalysis. Chem. Rev. *111*, 2119–2176.

47. Li, W., and Zhang, J. (2016). Recent developments in the synthesis and utilization of chiral β-aminophosphine derivatives as catalysts or ligands. Chem. Soc. Rev. *45*, 1657–1677.

48. Ni, H., Chan, W.-L., and Lu, Y. (2018). Phosphine-catalyzed asymmetric organic reactions. Chem. Rev. *118*, 9344–9411.

49. Guo, H., Fan, Y.C., Sun, Z., Wu, Y., and Kwon, O. (2018). Phosphine organocatalysis. Chem. Rev. *118*, 10049–10293.

50. Clevenger, A.L., Stolley, R.M., Aderibigbe, J., and Louie, J. (2020). Trends in the usage of bidentate phosphines as ligands in nickel catalysis. Chem. Rev. *120*, 6124–6196.

51. Xu, G., Senanayake, C.H., and Tang, W. (2019). P-chiral phosphorus ligands based on a 2,3-dihydrobenzo[d][1,3]oxaphosphole motif for asymmetric catalysis. Acc. Chem. Res. *52*, 1101–1112.

52. Join, B., Mimeau, D., Delacroix, O., and Gaumont, A.-C. (2006). Pallado-catalysed hydrophosphination of alkynes: access to enantio-enriched P-stereogenic vinyl phosphine–boranes. Chem. Commun. (Camb) *30*, 3249–3251.

53. Yang, Z., Gu, X., Han, L.-B., and Wang, J.J. (2020). Palladium-catalyzed asymmetric hydrophosphorylation of alkynes: facile access to P-stereogenic phosphinates. Chem. Sci. *11*, 7451–7455.

54. Dai, Q., Liu, L., Qian, Y., Li, W., and Zhang, J. (2020). Construction of P-chiral alkenylphosphine oxides through highly chemo-, regio-, and enantioselective hydrophosphinylation of alkynes. Angew. Chem. Int. Ed. Engl. *59*, 20645–20650.

55. Liu, X.-T., Han, X.-Y., Wu, Y., Sun, Y.-Y., Gao, L., Huang, Z., and Zhang, Q.-W. (2021). Ni-catalyzed asymmetric hydrophosphination of unactivated alkynes. J. Am. Chem. Soc. *143*, 11309–11316.

56. Feng, J.-J., Chen, X.-F., Shi, M., and Duan, W.-L. (2010). Palladium-catalyzed asymmetric addition of diarylphosphines to enones toward the synthesis of chiral phosphines. J. Am. Chem. Soc. *132*, 5562–5563.

57. Wang, C., Huang, K., Ye, J., and Duan, W.-L. (2021). Asymmetric synthesis of Pstereogenic secondary phosphine-boranes by an unsymmetric bisphosphine pincer-nickel complex. J. Am. Chem. Soc. *143*, 5685–5690.

58. Huang, Y., Pullarkat, S.A., Li, Y., and Leung, P.-H. (2010). Palladium(II)-catalyzed asymmetric hydrophosphination of enones: efficient access to chiral tertiary phosphines. Chem. Commun. (Camb) *46*, 6950–6952.

59. Li, Y.-B., Tian, H., and Yin, L. (2020). Copper(I)-catalyzed asymmetric 1,4-conjugate hydrophosphination of α,β-unsaturated amides. J. Am. Chem. Soc. *142*, 20098–20106.

60. Yue, W.-J., Xiao, J.-Z., Zhang, S., and Yin, L. (2020). Rapid synthesis of chiral 1,2-bisphosphine derivatives through copper(I)-catalyzed asymmetric conjugate hydrophosphination. Angew. Chem. Int. Ed. *59*, 7057–7062.

61. Ding, B., Zhang, Z., Xu, Y., Liu, Y., Sugiya, M., Imamoto, T., and Zhang, W. (2013). P-stereogenic PCP pincer–Pd complexes: synthesis and application in asymmetric addition of diarylphosphines to nitroalkenes. Org. Lett. *15*, 5476–5479.

62. Zhang, Y.-Q., Han, X.-Y., Wu, Y., Qi, P.-J., Zhang, Q., and Zhang, Q.-W. (2022). Ni-catalyzed asymmetric hydrophosphinylation of conjugated enynes and mechanistic studies. Chem. Sci. *13*, 4095–4102.

63. Pérez, J.M., Postolache, R., Castiñeira Reis, M.C., Sinnema, E.G., Vargová, D., de Vries, F., Otten, E., Ge, L., and Harutyunyan, S.R. (2021). Manganese(I)-catalyzed H−P bond activation via metal−ligand cooperation. J. Am. Chem. Soc. *143*, 20071–20076.

64. Ge, L., and Harutyunyan, S.R. (2022). Manganese(I)-catalyzed access to 1,2-bisphosphine ligands. Chem. Sci. *13*, 1307–1312.

65. Sadow, A.D., Haller, I., Fadini, L., and Togni, A. (2004). Nickel(II)-catalyzed highly enantioselective hydrophosphination of methacrylonitrile. J. Am. Chem. Soc. *126*, 14704–14705.

66. Sadow, A.D., and Togni, A. (2005). Enantioselective addition of secondary phosphines to methacrylonitrile: catalysis and mechanism. J. Am. Chem. Soc. *127*, 17012–17024.

67. Lu, Z., Zhang, H., Yang, Z., Ding, N., Meng, L., and Wang, J. (2019). Asymmetric hydrophosphination of heterobicyclic alkenes: facile access to phosphine ligands for asymmetric catalysis. ACS Catal. *9*, 1457–1463.

68. Long, J., Li, Y., Zhao, W., and Yin, G. (2022). Nickel/Brønsted acid dual-catalyzed regio- and enantioselective hydrophosphinylation of 1,3-dienes: access to chiral allylic phosphine oxides. Chem. Sci. *13*, 1390–1397.

69. Maiti, R., Yan, J.-L., Yang, X., Mondal, B., Xu, J., Chai, H., Jin, Z., and Chi, Y.R. (2021). Carbene-catalyzed enantioselective hydrophosphination of α-bromoenals to prepare phosphine-containing chiral molecules. Angew. Chem. Int. Ed. Engl. *60*, 26616–26621.

70. Nie, S.-Z., Davison, R.T., and Dong, V.M. (2018). Enantioselective coupling of dienes and phosphine oxides. J. Am. Chem. Soc. *140*, 16450–16454.

71. Xu, Q., and Han, L.-B. (2006). Palladium-catalyzed asymmetric hydrophosphorylation of norbornenes. Org. Lett. *8*, 2099–2101.

72. Ibrahem, I., Rios, R., Vesely, J., Hammar, P., Eriksson, L., Himo, F., and Córdova, A. (2007). Enantioselective organocatalytic hydrophosphination of α,β-unsaturated aldehydes. Angew. Chem. Int. Ed. Engl. *46*, 4507–4510.

73. Fu, X., Loh, W.-T., Zhang, Y., Chen, T., Ma, T., Liu, H., Wang, J., and Tan, C.-H. (2009). Chiral guanidinium salt catalyzed enantioselective phospha-Mannich reactions. Angew. Chem. Int. Ed. Engl. *48*, 7387–7390.

74. Khemchyan, L.L., Ivanova, J.V., Zalesskiy, S.S., Ananikov, V.P., Beletskaya, I.P., and Starikova, Z.A. (2014). Unprecedented control of selectivity in nickel-catalyzed hydrophosphorylation of alkynes: efficient route to mono- and bisphosphonates. Adv. Synth. Catal. *356*, 771–780.

75. Yang, Z., and Wang, J.J. (2021). Enantioselective palladium-catalyzed hydrophosphinylation of allenes with phosphine oxides: access to chiral allylic phosphine oxides. Angew. Chem. Int. Ed. Engl. *60*, 27288–27292.

76. Wu, Z.-H., Cheng, A.-Q., Yuan, M., Zhao, Y.-X., Yang, H.-L., Wei, L.-H., Wang, H.-Y., Wang, T., Zhang, Z., and Duan, W.-L. (2021). Cobalt-catalysed asymmetric addition and alkylation of secondary phosphine oxides for the synthesis of P-stereogenic compounds. Angew. Chem. Int. Ed. Engl. *60*, 27241–27246.

77. Huang, Y., Li, Y., Leung, P.-H., and Hayashi, T. (2014). Asymmetric synthesis of P-stereogenic diarylphosphinites by palladium-catalyzed enantioselective addition of diarylphosphines to benzoquinones. J. Am. Chem. Soc. *136*, 4865–4868.

78. Beaud, R., Phipps, R.J., and Gaunt, M.J. (2016). Enantioselective Cu-catalyzed arylation of secondary phosphine oxides with diaryliodonium salts toward the synthesis of P-chiral phosphines. J. Am. Chem. Soc. *138*, 13183–13186.

79. Zhang, Y., He, H., Wang, Q., and Cai, Q. (2016). Asymmetric synthesis of chiral P-stereogenic triaryl phosphine oxides via Pd-catalyzed kinetic arylation of diaryl phosphine oxides. Tetrahedron Lett. *57*, 5308–5311.

80. Dai, Q., Li, W., Li, Z., and Zhang, J. (2019). P-chiral phosphines enabled by palladium/Xiao-phos-catalyzed asymmetric P—C cross-coupling of secondary phosphine oxides and aryl bromides. J. Am. Chem. Soc. *141*, 20556–20564.

81. Liu, X.-T., Zhang, Y.-Q., Han, X.-Y., Sun, S.-P., and Zhang, Q.W. (2019). Ni-catalyzed asymmetric allylation of secondary phosphine oxides. J. Am. Chem. Soc. *141*, 16584–16589.

82. Duan, L., Zhao, K., Wang, Z., Zhang, F.-L., and Gu, Z. (2019). Enantioselective ring-opening/oxidative phosphorylation and P-transfer reaction of cyclic Diaryliodoniums. ACS Catal. *9*, 9852–9858.

83. Qiu, H., Dai, Q., He, J., Li, W., and Zhang, J. (2020). Access to P-chiral *sec*- and *tert*-phosphine oxides enabled by Le-Phos-catalyzed asymmetric kinetic resolution. Chem. Sci. *11*, 9983–9988.

84. Balázs, L.B., Huang, Y., Khalikuzzaman, J.B., Li, Y., Pullarkat, S.A., and Leung, P.-H. (2020). Catalytic asymmetric diarylphosphine addition to α-diazoesters for the synthesis of P-stereogenic phosphinates via P*-N bond formation. J. Org. Chem. *85*, 14763–14771.

85. Zhang, S., Xiao, J.-Z., Li, Y.-B., Shi, C.-Y., and Yin, L. (2021). Copper(I)-catalyzed asymmetric alkylation of unsymmetrical secondary phosphines. J. Am. Chem. Soc. *143*, 9912–9921.

86. Dai, Q., Liu, L., and Zhang, J. (2021). Palladium/Xiao-phos-catalyzed kinetic resolution of *sec*-phosphine oxides by *P*-benzylation. Angew. Chem. Int. Ed. Engl. *60*, 27247–27252.

87. Wang, H., Qian, H., Zhang, J., and Ma, S. (2022). Catalytic asymmetric axially chiral allenyl C–P bond formation. J. Am. Chem. Soc. *144*, 12619–12626. https://doi.org/10.1021/jacs.2c04931.

88. Cardoso, F.S.P., Abboud, K.A., and Aponick, A. (2013). Design, preparation, and implementation of an imidazole-based chiral biaryl P, N-ligand for asymmetric catalysis. J. Am. Chem. Soc. *135*, 14548–14551.

89. Li, X., Zhao, L., Qi, Z., and Li, X. (2021). Construction of atropisomeric 3-arylindoles via enantioselective Cacchi reaction. Org. Lett. *23*, 5901–5905.

90. Han, L.-B., and Tanaka, M. (1996). Palladium-catalyzed hydrophosphorylation of alkynes *via* oxidative addition of $HP(O)(OR)_2$. J. Am. Chem. Soc. *118*, 1571–1572.

91. Chen, T., Zhao, C.-Q., and Han, L.-B. (2018). Hydrophosphorylation of alkynes catalyzed by palladium: generality and mechanism. J. Am. Chem. Soc. *140*, 3139–3155.